Electronic Supplementary Material (ESI) for CrystEngComm.

Supporting Information

Peculiar Phenomena on Structural Transformation Triggered from A Nickel Coordination Polymer

Meng Kang, Guo-Ping Yang, Lei Hou, Wei-Ping Wu, Yun-Long Wu, Yao-Yu Wang*

Key Laboratory of Synthetic and Natural Functional Molecule Chemistry of the Ministry of Education, Shaanxi Key Laboratory of Physico-Inorganic Chemistry, College of Chemistry & Materials Science, Northwest University, Xi'an 710069, P. R. China.

E-mail: wyaoyu@nwu.edu.cn.

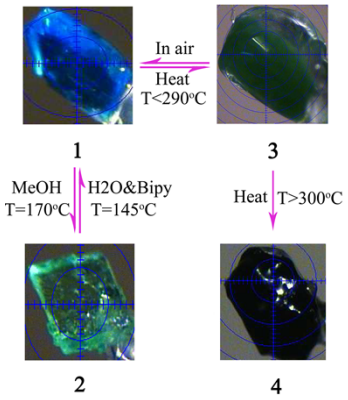

Fig. S1 View of the color changes of the four nickel-based CPs via structural transformation.

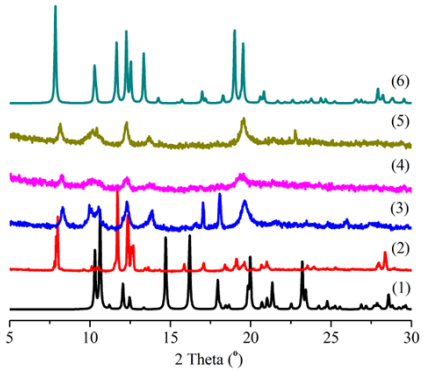

Fig. S2 View of the transformations of **1** to **2** in various solvents: PXRD patterns of as-simulated **1** (1), the activation of **1** at 170 °C in methanol (2), ethanol (3), *N,N′*-dimethylformamide (4) and acetonitrile (5), and as-simulated **2** (6).

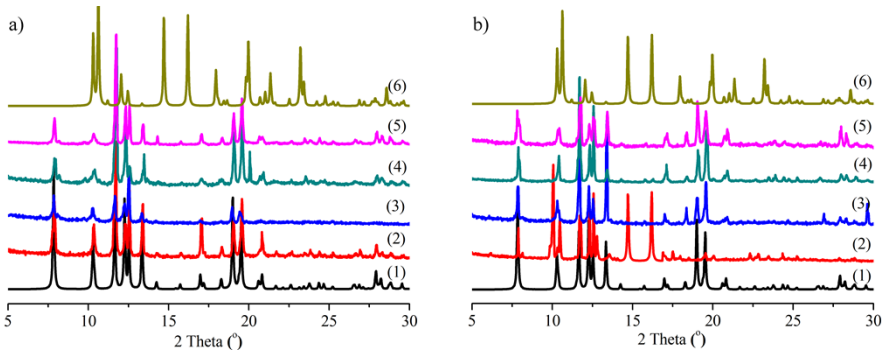

Fig. S3 View of the water-mediated transformation of **2** to **1** under the condition of adding bipy ligand: PXRD patterns of as-simulated **2** (1), the activation of **2** (a2) / **2&bipy** (b2) at 145 °C in water, methanol (3), acetonitrile (4) and *N,N′*-dimethylformamide (5), and as-simulated **1** (6).

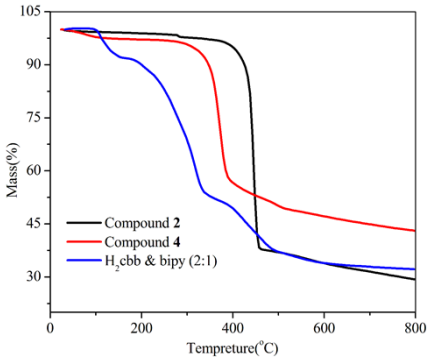

Fig. S4 View of the TGA plots of **2**, **4** and **H_2cbb & bipy (2:1)** in nitrogen stream.

TGA of **2** exhibits a plateau of stability up to 380 °C due to no coordinated solvent, then followed by a sharp weight loss induced by the decomposition of the framework. TGA of **4** indicates a preliminary weight loss of 2.7% (calc. 3.1%) from room temperature to 150 °C, corresponding to the release of water molecules, and then followed by a flat plateau from 150 to 350 °C. After that, a sharp weight loss is observed caused by the decomposition of the framework.

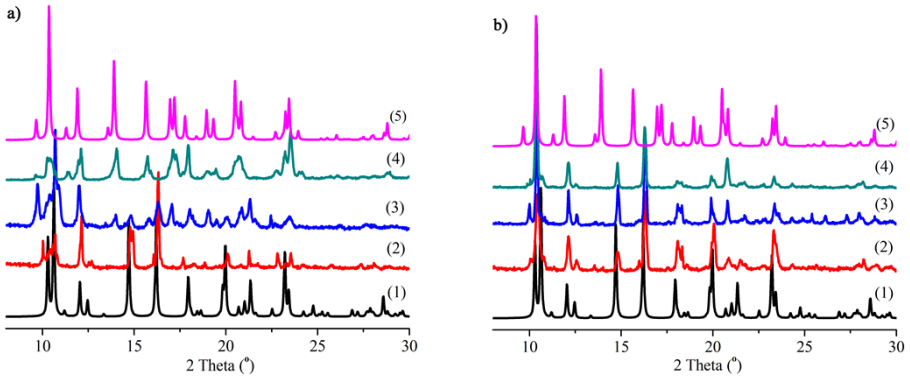

Fig. S5 View of the reversible solid-state SCSC transformation of **1** and **3**. (a) PXRD patterns of as-simulated **1** (1), the activation of **1** at 50 °C (2), 120 °C (3) and 210 °C (4), and as-simulated **3** (5). (b) PXRD patterns of as-simulated **1** (1), the exposure of activated-samples at 50 °C (2), 120 °C (3) and 210 °C (4) in air for 5 minutes, and as-simulated **3** (5).

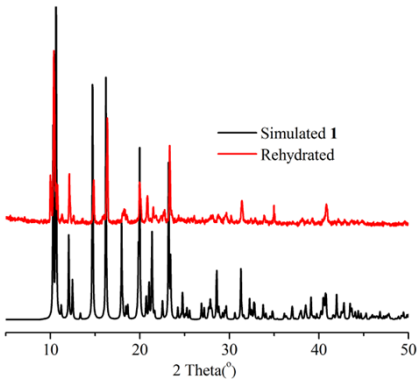

Fig. S6 The PXRD patterns of as-simulated **1** and the rehydrated sample after ten cycles of the reversible water uptake.

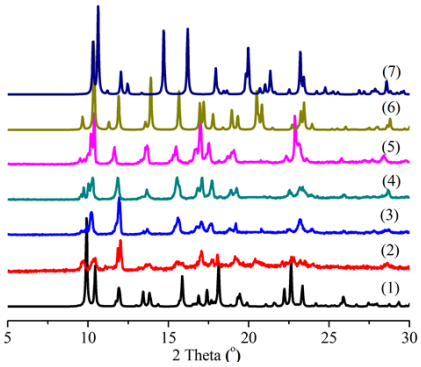

Fig. S7 PXRD patterns of as-simulated **4** (1), the activation of **4&cbb&bipy** at 170 °C in water (2), methanol (3), acetonitrile (4) and *N,N'*-dimethylformamide (5), as-simulated **3** (6) and as-simulated **1** (7).

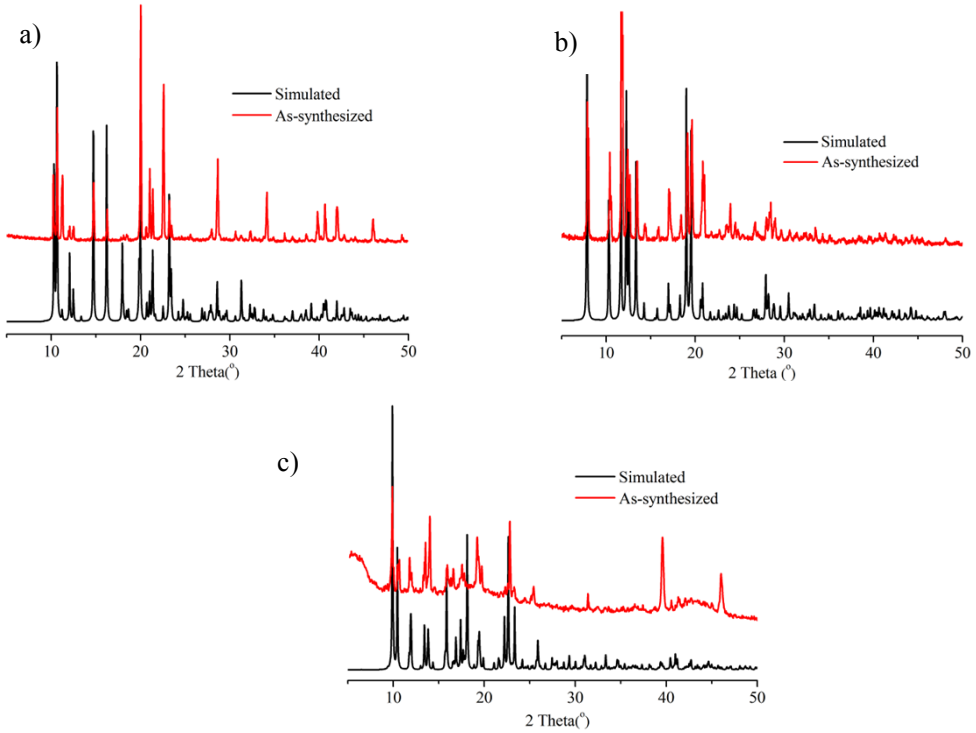

Fig. S8 The PXRD patterns of **1**(a), **2**(b) and **4**(c) simulated from the X-ray single-crystal structures and as synthesized samples.

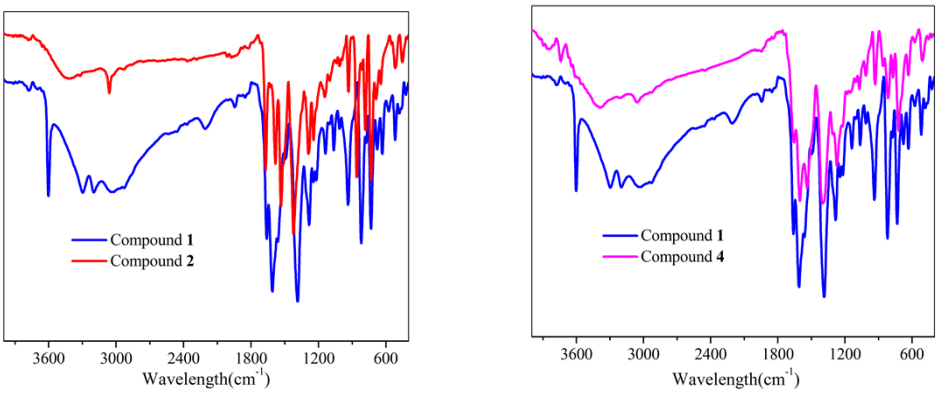

Fig. S9 View of the IR spectra of **1**, **2** and **4**.

Table S1. Selected Bond Lengths (Å) and Bond Angles (deg) for **1**-**4**.

Compound **1**			
Ni(1) -N(1)	2.084(5)	O(4)$^{\#3}$-Ni(1)-N(1)	178.2(2)
Ni(1) -N(2)	2.098(5)	O(2W)-Ni(1)-N(1)	88.7(2)
Ni(1)-O(1)	2.043(5)	O(1)-Ni(1)-N(2)	90.9(2)
Ni(1)-O(4)$^{\#3}$	2.061(4)	O(4)$^{\#3}$-Ni(1)-N(2)	89.3(2)
Ni(1)-O(2W)	2.067(4)	O(2W)-Ni(1)-N(2)	173.6(2)
Ni(1)-O(1W)	2.131(5)	N(1)-Ni(1)-N(2)	89.29(16)
Ni(1)$^{\#4}$-O(4)	2.061(4)	O(1)-Ni(1)-O(1W)	173.8(3)
O(1)-Ni(1)-O(4)$^{\#3}$	89.7(2)	O(4)$^{\#3}$-Ni(1)-O(1W)	84.31(19)
O(1)-Ni(1)-O(2W)	80.95	O(2W)-Ni(1)-O(1W)	86.88(19)
O(4)$^{\#3}$-Ni(1)-O(2W)	66.33	N(1)-Ni(1)-O(1W)	96.7(2)
O(1)-Ni(1)-N(1)	89.2(2)	N(2)-Ni(1)-O(1W)	87.3(2)

Symmetry transformations used to generate equivalent atoms: #1 x - 1/2, -y + 5/2, z - 1/2; #2 x + 1/2, -y + 5/2, z + 1/2; #3 x + 1, y, z; #4 x - 1, y, z.

Compound **2**			
Ni(1) -N(1)	2.032(7)	O(1)-Ni(1)-O(5)$^{\#3}$	87.2(3)
Ni(1)-O(1)	2.003(6)	O(4)$^{\#2}$-Ni(1)-O(5)$^{\#3}$	165.8(2)
Ni(1)-O(4)$^{\#2}$	2.005(6)	O(1)-Ni(1)-O(2)$^{\#4}$	166.0(3)
Ni(1)-O(5)$^{\#3}$	2.005(6)	O(4)$^{\#2}$-Ni(1)-O(2)$^{\#4}$	87.4(3)
Ni(1)-O(2)$^{\#4}$	2.025(6)	O(5)$^{\#3}$-Ni(1)-O(2)$^{\#4}$	90.5(3)
Ni(1)$^{\#4}$-O(2)	2.025(6)	O(1)-Ni(1)-N(1)	99.6(3)
Ni(1)$^{\#2}$-O(4)	2.005(6)	O(4)$^{\#2}$-Ni(1)-N(1)	98.3(3)
Ni(1)$^{\#5}$-O(5)	2.005(6)	O(5)$^{\#3}$-Ni(1)-N(1)	95.9(3)
O(1)-Ni(1)-O(4)$^{\#2}$	91.5(3)	O(2)$^{\#4}$-Ni(1)-N(1)	94.4(3)

Symmetry transformations used to generate equivalent atoms: #1 –x + 1, -y + 2, -z + 2; #2 -x + 2, -y + 1, -z + 1; #3 x, y + 1, z; #4 –x + 2, -y + 2, -z + 1; #5 x, y - 1, z.

Compound **3**			
Ni(1) -N(1)	2.096(7)	O(5)$^{\#4}$-Ni(1)-O(1)	90.6(2)
Ni(1) -N(2)	2.047(7)	N(1)-Ni(1)-O(1)	96.3(3)
Ni(1)-O(5)$^{\#4}$	2.078(6)	N(2)-Ni(1)-O(2)	94.1(3)
Ni(1)-O(1)	2.141(5)	O(5)$^{\#4}$-Ni(1)-O(2)	89.2(2)
Ni(1)-O(2)	2.165(7)	N(1)-Ni(1)-O(2)	157.4(3)
Ni(1)-O(4)$^{\#4}$	2.201(6)	O(1)-Ni(1)-O(2)	61.0(2)
O(4)-Ni(1)$^{\#1}$	2.201(6)	N(2)-Ni(1)-O(4)$^{\#4}$	110.8(3)
O(5)-Ni(1)$^{\#1}$	2.078(6)	O(5)$^{\#4}$-Ni(1)-O(4)$^{\#4}$	61.4(2)
N(2)-Ni(1)-O(5)$^{\#4}$	171.5(3)	N(1)-Ni(1)-O(4)$^{\#4}$	112.1(3)
N(2)-Ni(1)-N(1)	89.6(3)	O(1)-Ni(1)-O(4)$^{\#4}$	139.0(2)

O(5)$^{\#4}$-Ni(1)-N(1)	90.4(3)	O(2)-Ni(1)-O(4)$^{\#4}$	87.4(3)
N(2)-Ni(1)-O(1)	97.8(3)		

Symmetry transformations used to generate equivalent atoms: #1 x - 1, y, z; #2 x + 1/2, -y + 5/2, z + 1/2; #3 x - 1/2, -y + 5/2, z - 1/2; #4 x + 1, y, z.

Compound **4**			
Ni(1)$^{\#1}$-O(4)	1.997(3)	N(1)-Ni(1)-O(2)	159.45(12)
Ni(1)-O(4)$^{\#1}$	1.997(3)	N(2)$^{\#2}$-Ni(1)-O(2)	87.36(11)
Ni(1)-N(1)	2.077(3)	O(4)$^{\#1}$-Ni(1)-N(3)	87.35(12)
Ni(1)-N(2)$^{\#2}$	2.114(3)	N(1)-Ni(1)-N(3)	93.69(12)
Ni(1)-O(2)	2.117(3)	N(2)$^{\#2}$-Ni(1)-N(3)	173.74(12)
Ni(1)-N(3)	2.143(3)	O(2)-Ni(1)-N(3)	86.55(12)
Ni(1)-O(1)	2.179(3)	O(4)$^{\#1}$-Ni(1)-O(1)	157.07(12)
N(2)-Ni(1)$^{\#3}$	2.114(3)	N(1)-Ni(1)-O(1)	97.88(12)
O(4)$^{\#1}$-Ni(1)-N(1)	105.04(13)	N(2)$^{\#2}$-Ni(1)-O(1)	87.96(13)
O(4)$^{\#1}$-Ni(1)-N(2)$^{\#2}$	91.81(12)	O(2)-Ni(1)-O(1)	61.57(11)
N(1)-Ni(1)-N(2)$^{\#2}$	92.52(13)	N(3)-Ni(1)-O(1)	90.40(13)
O(4)$^{\#1}$-Ni(1)-O(2)	95.51(12)		

Symmetry transformations used to generate equivalent atoms: #1 –x + 2, y, -z + 3/2; #2 x + 1/2, -y + 1/2, z + 1/2; #3 x - 1/2, -y + 1/2, z - 1/2; #4 –x + 1, -y + 1, -z + 1.